Electrical Stimulation of Pediatric Cardiac-Derived c-kit+ Progenitor Cells Improves Retention and Cardiac Function in Right Ventricular Heart Failure

JOSHUA T. MAXWELL [ID],[a,b] DAVID TRAC,[c] MING SHEN,[a,b] MILTON E. BROWN,[c]
MICHAEL E. DAVIS,[a,b,c] MYRA S. CHAO,[d] KRITTIN J. SUPAPANNACHART,[e] CARLY A. ZALADONIS,[d]
EMILY BAKER,[d] MARTIN L. LI,[d] JENNIFER ZHAO,[f] DANIEL I. JACOBS[d]

Key Words. Heart failure • Heart defects, congenital • Stem cells • Humans • Cell- and tissue-based therapy • Electrical stimulation

aDivision of Pediatric Cardiology, Department of Pediatrics, Emory University School of Medicine, Atlanta, Georgia, USA; bChildren's Heart Research & Outcomes (HeRO) Center, Children's Healthcare of Atlanta & Emory University, Atlanta, Georgia, USA; cWallace H. Coulter Department of Biomedical Engineering, Georgia Institute of Technology & Emory University School of Medicine, Atlanta, Georgia, USA; dEmory University College of Arts and Sciences, Atlanta, Georgia, USA; eEmory University School of Medicine, Atlanta, Georgia, USA; fCornell University College of Arts and Sciences, Ithaca, New York, USA

Correspondence: Joshua T. Maxwell, Ph.D., Emory University School of Medicine, Atlanta, Georgia 30322, USA. Telephone: 404-727-4441; e-mail: jtmaxwe@emory.edu

ABSTRACT

Nearly 1 in every 120 children born has a congenital heart defect. Although surgical therapy has improved survival, many of these children go on to develop right ventricular heart failure (RVHF). The emergence of cardiovascular regenerative medicine as a potential therapeutic strategy for pediatric HF has provided new avenues for treatment with a focus on repairing or regenerating the diseased myocardium to restore cardiac function. Although primarily tried using adult cells and adult disease models, stem cell therapy is relatively untested in the pediatric population. Here, we investigate the ability of electrical stimulation (ES) to enhance the retention and therapeutic function of pediatric cardiac-derived c-kit+ progenitor cells (CPCs) in an animal model of RVHF. Human CPCs isolated from pediatric patients were exposed to chronic ES and implanted into the RV myocardium of rats. Cardiac function and cellular retention analysis showed electrically stimulated CPCs (ES-CPCs) were retained in the heart at a significantly higher level and longer time than control CPCs and also significantly improved right ventricular functional parameters. ES also induced upregulation of extracellular matrix and adhesion genes and increased in vitro survival and adhesion of cells. Specifically, upregulation of β1 and β5 integrins contributed to the increased retention of ES-CPCs. Lastly, we show that ES induces CPCs to release higher levels of pro-reparative factors in vitro. These findings suggest that ES can be used to increase the retention, survival, and therapeutic effect of human c-kit+ progenitor cells and can have implications on a variety of cell-based therapies. STEM CELLS 2019;37:1528–1541

SIGNIFICANCE STATEMENT

Cardiac-derived progenitor cells (CPCs) have been widely studied as a cell-based therapy for cardiac pathologies; however, unless these cells are extracted at a very young age, their therapeutic efficacy is diminished. Finding novel ways to enhance the reparative potential of these cells is thus of critical significance. It is shown that electrical stimulation of pediatric CPCs can induce them to have a beneficial effect on failing heart function. These findings present a method for enhancing the reparative ability of CPCs and also provide insights into the mechanism of enhanced function that can be translated to other cell-based therapies.

INTRODUCTION

Nearly 1% of babies born in the U.S. will be diagnosed with a congenital heart defect (CHD). CHDs are the most common birth defect and are the number one cause of death from birth defects during the first year of life [1]. CHDs are the leading cause of right ventricular heart failure (RVHF) in the pediatric population, especially in patients with defects like pulmonary stenosis, Hypoplastic Left Heart Syndrome and Tetrology of Fallot [2]. There is much evidence on the differences between the right and left ventricle in both structure, function, and pathologies [3, 4]. Undoubtedly, these differences have consequences for the evaluation and treatment strategy for patients with predominantly right, left, or biventricular HF [5], and generalizing heart failure treatments and attempting to extrapolate data and experience from LV failure to RV failure are futile. Current therapeutics for RV failure including pharmacological agents, further surgical or mechanical interventions, and eventually heart

transplantation at the end stage of HF make the clinical management of patients with RV failure both costly and challenging [5].

The recent emergence of stem cell-based myocardial repair for the treatment of HF has provided an alternative approach [6]. One such cell, known as CPCs, is an excellent choice for cell-based therapies for children because they can be easily isolated, exponentially expanded ex vivo while maintaining their stemness, and provides an excellent autologous and allogeneic therapeutic tool for treating various heart diseases. However, we have shown in a recent publication that CPCs lose their therapeutic functionality as they age. Unless these cells are extracted at a very young age (<1 year), the therapeutic efficacy of CPCs is diminished [7]. Finding novel ways to enhance the reparative potential of these cells would overcome this critical barrier to stem cell therapy, allow for both autologous and allogeneic treatment options in children and adults, and could be extended to other stem cell types [8–12].

Several laboratories have demonstrated the feasibility and utility of ex vivo manipulation of adult stem cells modified by genetic engineering [13–17] or exposure to environmental, chemical, and biological treatments prior to delivery [13, 18–21]. The idea behind these strategies is to isolate a patient's CPCs and expand and modify them to create a more reparative phenotype. Electrical stimulation (ES) is one treatment that has been shown to induce differentiation, enhance survival, and promote function of cardiac stem cells isolated from animals; however, the effect of ES on human CPCs (adult or pediatric) has yet to be examined [22–26].

Our previously published data show that pediatric CPCs (isolated from patients between 1 and 5 years of age) respond to ES by initiating calcium (Ca^{2+}) oscillations making them an ideal population of cells for manipulation by ex vivo ES [27]. Therefore, we sought to investigate the ability of ES to modulate the therapeutic efficacy of CPCs in an animal model of juvenile RVHF. Here, we show that ES improves CPC function, retention, and survival. We found that upregulation of integrins β1 and β5 contribute to the increased in vivo retention of ES-CPCs. We also present an insight into the mechanism of CPC modification that has implications on a variety of stem cells and stem cell therapies.

MATERIALS AND METHODS

Human Sample Acquisition and Isolation of Human CPCs

This study was approved by the Institutional Review Board at Children's Healthcare of Atlanta and Emory University. Approximately 100 mg of right atrial appendage tissue was obtained from children undergoing reconstructive surgeries. Child CPCs are categorized as being isolated from patients aged 12 months to 5 years. Neonatal CPCs were also used in some experiments and are categorized as being isolated from patients aged 1 week to 1 month. CPCs were isolated within 4 hours of sample acquisition as previously described [28]. Atrial tissue was transported to the laboratory in Krebs-Ringer solution containing 35 mM NaCl, 4.75 mM KCl, 1.2 mM KH2PO4, 16 mM Na2HPO4, 134 mM sucrose, 25 mM NaHCO3, 10 mM glucose, 10 mM HEPES, and 30 mM 2,3-butanedione monoxime, pH = 7.4 with NaOH.

CPC Culture and Electrical Stimulation

CPCs were maintained in culture in Ham's F12 medium supplemented with 10% of fetal bovine serum (FBS), 100 U/ml of penicillin/streptomycin, 2 mmol/l of L-glutamine, and 0.01 μg/ml of basic fibroblast growth factor (bFGF). For ES of CPCs, cells were seeded onto 6-well dishes at ∼1,000,000 cells per well in calcium-supplemented media (CPC culture media plus 2 mmol/l CaCl$_2$). A C-dish electrode array in conjunction with C-Pace Electrical Stimulation System (Ion Optix) was used to apply chronic electrical pulses to the cells at 1 Hz frequency, 10 ms duration, and 10 V amplitude for 7 or 14 days. Media was replaced every 24–48 hours. Control CPCs were cultured in calcium supplemented media for 7 days.

Flow Cytometry Analysis

CPCs were passaged 3–5 times, fixed with 2% paraformaldehyde, and stained for c-kit (H-300; Santa Cruz Biotechnology, Dallas TX), GATA-4 (9,053; Santa Cruz Biotechnology), and Nkx-2.5 (14,033; Santa Cruz Biotechnology), Notch1 (ab8925, Abcam, Cambridge, UK), Sca-1 (ab51317, Abcam), CD31 (sc-28,188, Santa Cruz Biotechnology), or CD34 (7,324; Santa Cruz Biotechnology). Pooled patient cell lines were used, and the data were analyzed using Flow Jo V10 software. Cells were also analyzed before after ES with Ki-67 antibody (sc-23,900, Santa Cruz Biotechnology) and Calcein AM and Ethidium homodimer-1 for live/dead quantification in addition to microscopy.

Intracellular Calcium Measurements

Prior to experiments, cells were plated on glass coverslips and allowed to attach overnight at 37°C. Cells were loaded with 10 μMfluo-4/AM for 20 minutes followed by a 20-minute wash in Tyrode's solution for de-esterification of the dye. Electrical field stimulation was applied using an IonOptix MyoPacer Cell Stimulator (10 ms duration, 32 V) and fluo-4 was excited at 488 nm and emission collected at 515 ± 15 nm using laser scanning confocal microscopy (FV1000). Calcium oscillation measurements were acquired from CPCs during 0.5 or 1 Hz stimulation bathed in Tyrode's solution, which contained (in mM) 130 NaCl, 4 KCl, 2 CaCl2, 1 MgCl2, 10D-glucose, and 10 Hepes, pH 7.4 with NaOH. All experiments were performed at room temperature (20°C–24°C). Data were analyzed using Olympus FV1000 FluoView software and Fiji.

Rat Pulmonary Artery Banding Model

All animal experiments were performed with the approval of the Institutional Animal Care and Use Committee of Emory University. Male adolescent (6 weeks old) athymic rats (Crl: NIH-Foxn1^{rnu}) (∼150 g) were obtained from Charles River Laboratories (Wilmington, MA). All rats exhibited normal RV function on echocardiography at the time of pulmonary artery banding (PAB) surgery (7–8 weeks old). Rats were anesthetized with 2% isoflurane, USP (Piramal Healthcare, Boston, MA), and a limited left thoracotomy was performed to expose the pulmonary artery (PA). The PA was dissected from the aorta and partially ligated over an 18-gauge angiocatheter. The sizer was then promptly removed to allow for antegrade flow through the banded area, and thoracotomy performed was closed under positive pressure ventilation to evacuate pleural air. Sham animals underwent the same procedure without banding

the PA. All animals were assigned an animal study number. Animals were randomly assigned to treatment groups using simple randomization with computer-generated random numbers. Once a treatment group reached capacity, that treatment group was removed from the randomization scheme. There were no significant differences in animal weights between treatment groups. All researchers performing echo-guided injections, echocardiograms, whole-animal in vivo imaging, histological analyses, or data analyses were blinded to the treatments. The study was unblinded after the collection and analyses of all data.

Cell Labeling, Delivery, and In Vivo Imaging

Control and ES-CPCs were harvested in phosphate-buffered saline (PBS) containing 5 mM EDTA and labeled with DiR (Thermo Fisher Scientific Life Sciences, Waltham, MA) per manufacturer's protocol, which fluoresces at near-infrared wavelengths. A total of 500,000 DiR-labeled cells were resuspended in 50 µl of saline and injected under echocardiographic guidance into the RV free wall using a 27-gauge BD Insulin Syringe with 12.7 mm BD Micro-Fine short bevel needle mounted on a stereotactic frame (BD Medical Technology). Successful delivery of CPCs into the rat myocardium was confirmed by echocardiography. The rats were imaged on days 0, 3, 7, 14, 21, 28, 35, and 42 using an IVIS Spectrum in vivo imager (Perkin Elmer, Waltham, MA). DiR fluorescence in the rat heart was measured as radiant efficiency and compared between rats as percentage retention (100% on day 0) over time.

Echocardiography

Transthoracic echocardiography was performed using a Vevo 2100 digital high-frequency ultrasound system (FujiFilm Visualsonics, Toronto, ON, Canada) equipped with a probe (MS250) suited for rat imaging. Tricuspid annular plane systolic excursion (TAPSE) was measured in the apical four-chamber view in M-mode. RV end diastolic and end systolic two-dimensional areas were measured in the apical four-chamber view in B-mode and RV fractional area change was calculated as $\frac{end\ diastolic\ area - end\ systolic\ area}{end\ diastolic\ area}$. RV end diastolic diameter (RVEDD) was measured from the interventricular septum to the RV free wall in the apical four-chamber view in B-mode. RV wall thickness was measured in the two-dimensional short-axis view in M-mode.

Fibrosis Analysis

Picrosirius staining was performed for collagen assessment. Briefly, heart tissue sections were washed in 1× PBS to remove optimal cutting temperature (OCT) medium followed by incubation with Picrosirius solution (1 g/l Sirius red F3B in saturated picric acid solution). The sections were washed with dilute acetic acid followed by ethanol and mounted with Cytoseal (Thermo Fisher Scientific Life Sciences). Images were taken using a Hamamatsu NanoZoomer S210 slide scanner (Hamamatsu Photonics, Hamamatsu City, Japan). Fibrotic area was quantified using ImageJ with Threshold Color plugin (G. Landini software, http://www.mecourse.com/landinig/software/software.html), and percentage fibrosis was calculated as $\frac{fibrotic\ area\ in\ RV}{total\ area\ of\ RV}$.

Immunostaining

Rats were sacrificed at day 42 after cell injections. Hearts were harvested en bloc fixed in 10% neutral buffered formalin for 4 hours, cryoprotected in 30% sucrose overnight, and embedded in OCT medium. Immunostaining was performed per protocol. In brief, 5-µm-thick tissue sections were prepared starting at the heart apex using a Cryotome FSE Cryostat (Thermo Fisher Scientific Life Sciences). Tissue sections were cleared of OCT medium by washing in 1× PBS and then blocked with 3% bovine serum albumin containing 0.02% sodium azide and 0.1% Triton X-100. Tissue sections were incubated with Alexa Fluor-conjugated primary antibodies overnight at 4°C. Conjugated antibodies used were human-specific Ku86 conjugated to Alexa Fluor 647 (sc-5280; Santa Cruz Biotechnology) and PECAM1 conjugated to Alexa Fluor 568 (sc-376764; Santa Cruz Biotechnology). All experiments performed included sections from control hearts incubated with the above-conjugated antibodies. All sections were mounted with Vectashield antifade mounting medium with DAPI (Vector Laboratories) before imaging with an Olympus IX81 FluoView FV1000 confocal microscope. Ki-67 antibody (sc-23900; Santa Cruz Biotechnology) was used along with AF-488 secondary antibody to stain CPCs fixed in 4% paraformaldehyde (See Supporting Information Fig. S1).

Quantitative Real-Time PCR

Total RNA was extracted from cell homogenates using TRIzol reagent (Invitrogen, Carlsbad, CA) per manufacturer's protocol, followed by DNase I treatment and first-strand cDNA synthesis with M-MLV reverse transcriptase (Invitrogen) primed by random hexamers and oligo(dT)18. Real-time PCR was then performed on the StepOne Plus System (Applied Biosystems, Foster City, CA) based on SYBR Green fluorescence detection of PCR products. Primer sequences are listed in Table 1.

Profiling of Extracellular Matrix and Adhesion Molecules

Extracellular Matrix and Adhesion Molecules RT2 Profiler real-time PCR-based 84 gene array (Qiagen, Hilden, Germany, PAHS-013Z) was used for profiling extracellular matrix and adhesion molecules. The data obtained were confirmed by qRT-PCR for Has1, Mmp9, Col14A1, Thbs3, and Itgb5 using specific primers (Integrated DNA Technologies, Coralville, IA).

Integrin Expression Analysis

Protein expression was measured using colorimetric α/β integrin-mediated cell adhesion array (EMD Millipore, Burlington, MA, ECM532), following the manufacturer's protocol. Briefly, cells were dislodged from tissue culture flasks using PBS + 5 mM EDTA and integrin surface expression measured using ELISA array plates read using a plate reader (Biotek Synergy2, Winooski, VT).

Lentiviral shRNA Transduction

Long-term and specific β1 or β5 integrin expression inhibition was produced by transducing CPCs with β1- or β5-shRNA (Santa Cruz Biotechnology, Dallas, TX) per manufacturer's protocol. CPCs underwent transduction and selection before ES.

Live-Dead Assay

CPCs were incubated with 2 µg/ml of Calcein AM and 4 µg/ml of Ethidium homodimer-1 (Thermo Fisher Scientific Life

Table 1. Quantitative real-time polymerase chain reaction primer sequences

Gene Name	Forward	Reverse
HAS1	CAT AGG AGG CAG TTT AGC GTA G	CCC AAG GTC ACT CAG GTA ATA AG
MMP14	GCT GAG AGA AGG ATG GGA ATA G	GCG CCT GGT ATG TGG TAT TA
THBS3	TGG GAC CCT TGT GAT GAA TG	CTA TGG TGG GTC TCC TCA GAT A
COL14A1	GGC CTT CCT TTC CTC TTA TCT G	CTT TCT CTC TCC CTC TCC TTC T
ITGB5	CCT GGC CTG CTT CTC ATT TA	GGA GAG CCT TCA CAC AAG ATA G
ITGB1	TGA TCC TGT GTC CCA TTG TAA G	TGA CCT CGT TGT TCC CAT TC
ACTA-2	AAT ACT CTG TCT GGA TCG GTG GCT	ACG AGT CAG AGC TTT GGC TAG GAA
vWF	TGT CTG GCT GAG GGA GGT AA	GTA CAT GGC TTT GCT GGC AC
veCAD	TTT CCA GCA GCC TTT CTA CCA	GGA AGA ACT GGC CCT TGT CA
Flt-1	GAC TAG ATA GCG TCA CCA GCA G	GAA ACC GTC AGA ATC CTC CTC
WT-1 (Wilm's Tumor 1)	GCA TCT GAG ACC AGT GAG AAA	TCC TGC TGT GCA TCT GTA AG
CD31	TCT ATG ACC TCG CCC TCC ACA AA	GAA CGG TGT CTT CAG GTT GTT ATT T CA
CD44	GCA GGT ATG GGT TCA TAG AAG G	GGT GTT GGA TGT GAG GAT GT
CD105	GCA GGT GTC AGC AAG TAT GA	GAA AGA GAG GCT GTC CAT GTT
E-Cadherin	GTC ATT GAG CCT GGC AAT TTA G	GTT GAG ACT CCT CCA TTC CTT C
GATA4	GGA GAT GCG TCC CAT CAA GAC	GGA GAC GCA TAG CCT TGT GG
NKX2.5	ACC TGA GTC CCT CTG GAT TT	TCA CTC ATT GCA CGC TGC AT
MEF2C	TAA CTT CTT TTC ACT GTT GTG CTC CTT	GCC GCT TTT GGC AAA TGT T
Cav1.2	GGC AGA GTG GTA GGT GAT AAA G	CCA TAA ATG ACT GCA AGC ATC G
IP3R1	AGT GAG AAA TGG GCT GGT AAA GT	CTT ATC CCA GAC CAA GAA TCG G
SERCA2a	TAG AGA TGA GGG TCT CGC TAT G	TTA TAG GCA TGA GCC ACT GTT C
GAPDH	GTG GAC CTG ACC TGC CGT CT	GGA GGA GTG GGT GTC GCT GT

The sequence of the forward and reverse primers used in the study are listed above. Primers were created using Integrated DNA Technology Primer Quest online tool against human gene sequences.

Sciences) per manufacturer's protocol. CPCs were imaged in solution using an Olympus IX81 FluoView FV1000 confocal microscope. Fluorescence images were obtained from randomly selected microscopic fields at 10× magnification. Percentage of live cells was quantified using ImageJ (Fiji).

Cell Adhesion Analysis

Cell adhesion assay was performed using CytoSelect 48-well cell adhesion assay ECM array (Cell Biolabs, San Diego, CA) per manufacturer's instruction. Briefly, CPCs were subjected to 7-day ES as described above or cultured in calcium supplemented media (control). Subsequently, cells received no treatment, passage through a 27-gauge needle, or were exposed to 300 µM H_2O_2 for 5 hours. After washing with PBS, lysis buffer/cytoquant GR dye reagent (Molecular Probes, OR) was applied to the cells for 20 minutes. Fluorescence intensity was measured using a plate reader with excitation set at 485 nm and emission detection at 530 nm.

Luminex Multiplex Immunoassay

CPC conditioned media was produced by culturing 60%–80% confluent control or ES-CPCs in media devoid of FBS and bFGF for 12 hours. The levels of specific secreted factors in CPC conditioned media were determined using a custom Luminex multiplex immunoassay to quantify the concentrations of angiogenin, bFGF, matrix metalloproteinase-9 (MMP-9), vascular endothelial growth factor (VEGF), hepatocyte growth factor (HGF), and interleukin 2 (IL-2). Data were normalized to total protein concentration as determined by BCA assay.

Statistical Analysis

Data are presented as mean ± SD unless otherwise noted in the legend. Statistical analysis was performed using Student's *t* test or analysis of variance.

RESULTS

ES-CPC Characterization

Populations of cells were isolated and expanded from right atrial appendage tissue from child donors (aged 12 months to 5 years) by c-kit$^+$ magnetic bead sorting. Prior characterization by flow cytometry showed these cells to be >95% positive for c-kit, Nkx2.5, and Gata4 (see Supporting Information Fig. S1A and Ref. [7]), and RT-PCR showed expression of multiple genes associated with an endothelial lineage (Supporting Information Fig. 1B) as recently reported [29]. CPCs were cultured in calcium supplemented media in the presence of ES (1 Hz, 10 mV, 10 ms). Electrically stimulated CPCs (ES-CPCs) were harvested and characterized. We have previously reported that ES of CPCs at these parameters initiates intracellular calcium oscillations in these cells [27] and causes Ca^{2+}-dependent changes in gene expression (Supporting Information Fig. 1C). In the prior study, we found 1 Hz to produce the maximal changes in intracellular Ca^{2+}, while having no negative effects on cell survival [27]. It was shown recently that CPCs lose their therapeutic functionality as they age. Unless these cells are extracted at a very young age (<1 year), the
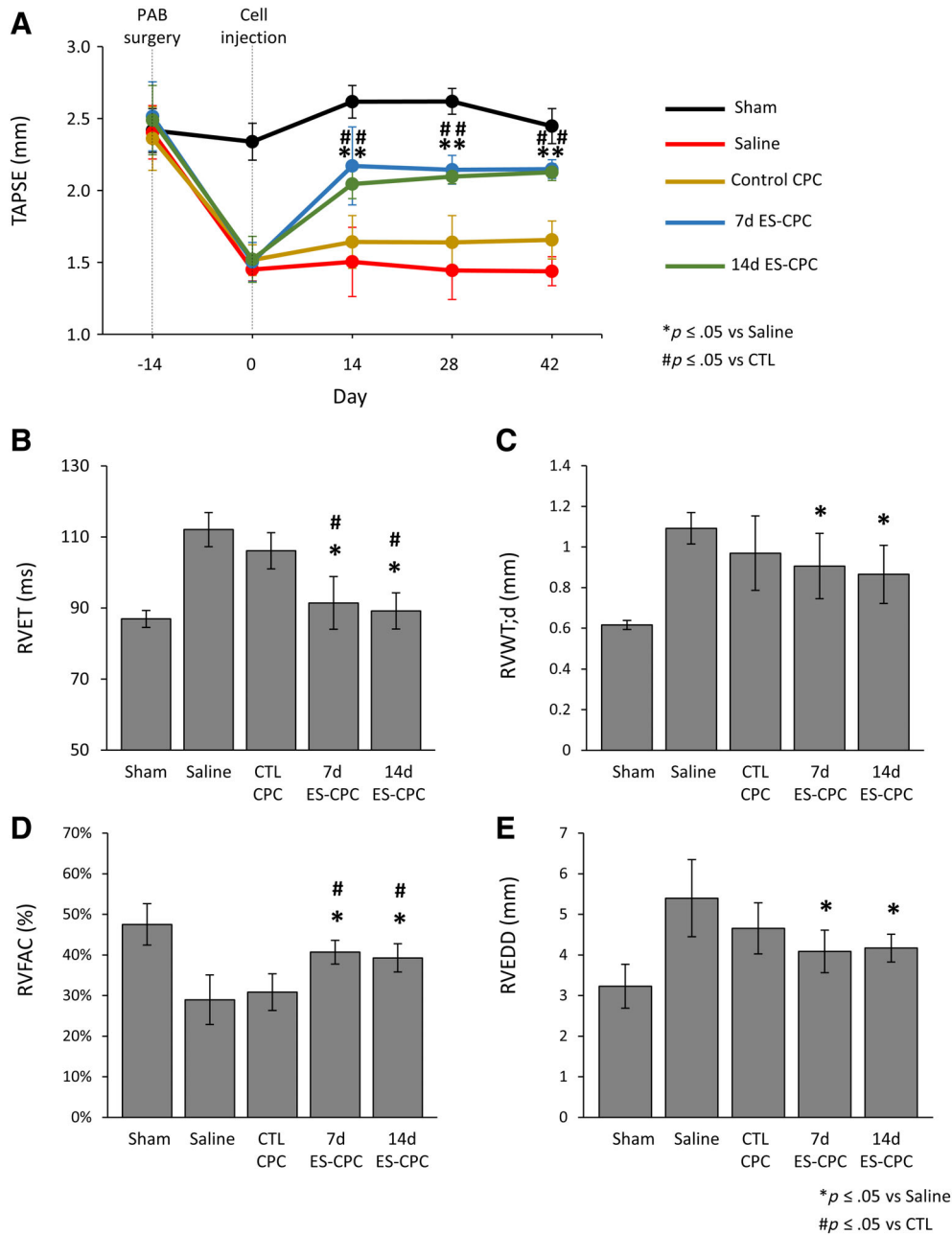
Figure 1. ES-CPCs significantly improve RV function in PAB rats. **(A):** Summary time course data of tricuspid annular plane systolic excursion (TAPSE) measurements in sham and PAB rats with injection of CPCs. Summary graphs of **(B)** right ventricle ejection time (RVET), **(C)** right ventricle wall thickness (RVWT), **(D)** right ventricle fractional area change (RVFAC), and **(E)** right ventricle end diastolic diameter (RVEDD) measured at day 42. $n = 5$ (sham), $n = 5$ (saline), $n = 9$ (control CPCs), $n = 9$ (7-day), $n = 7$ (14-day) for **(A)–(E)**. **(F):** Representative images of picrosirius red-stained fibrosis in rat heart sections. Dashed line indicates the areas used to quantify right ventricular free wall fibrosis. **(G):** Summary graph of fibrosis quantification in rat heart sections at day 42. $n = 5$ (sham), $n = 5$ (saline), $n = 9$ (control CPCs), $n = 9$ (7-day), $n = 7$ (14-day) for **(F)** and **(G)**. Data are presented as mean $\pm$ SD. *, $p \leq .05$ vs. saline; #, $p \leq .05$ vs control CPC. Abbreviations: CPCs, cardiac-derived c-kit$^+$ progenitor cells; ES-CPCs, electrically stimulated CPCs; PAB, pulmonary artery banding; RV, right ventricle.

therapeutic efficacy of CPCs is diminished [7]. Finding novel ways to enhance the reparative potential of these cells would overcome this critical barrier to stem cell therapy, allow for both autologous and allogeneic treatment options in children and adults, and could be extended to other stem cell types [8–12]. Based on previous work in other types of stem cells [22–26], we hypothesized that these Ca^{2+} oscillations could

induce changes in gene expression that would improve the therapeutic efficacy of these cells. We first examined the effect of ES on CPC proliferation using antibodies directed against the cell cycle protein Ki-67. Supporting Information Figure S2 shows Ki-67 staining-consistent with a progressive exit from the cell cycle after ES. This is a critical aspect of cell therapy, as implantation of proliferating cells could lead to teratoma formation
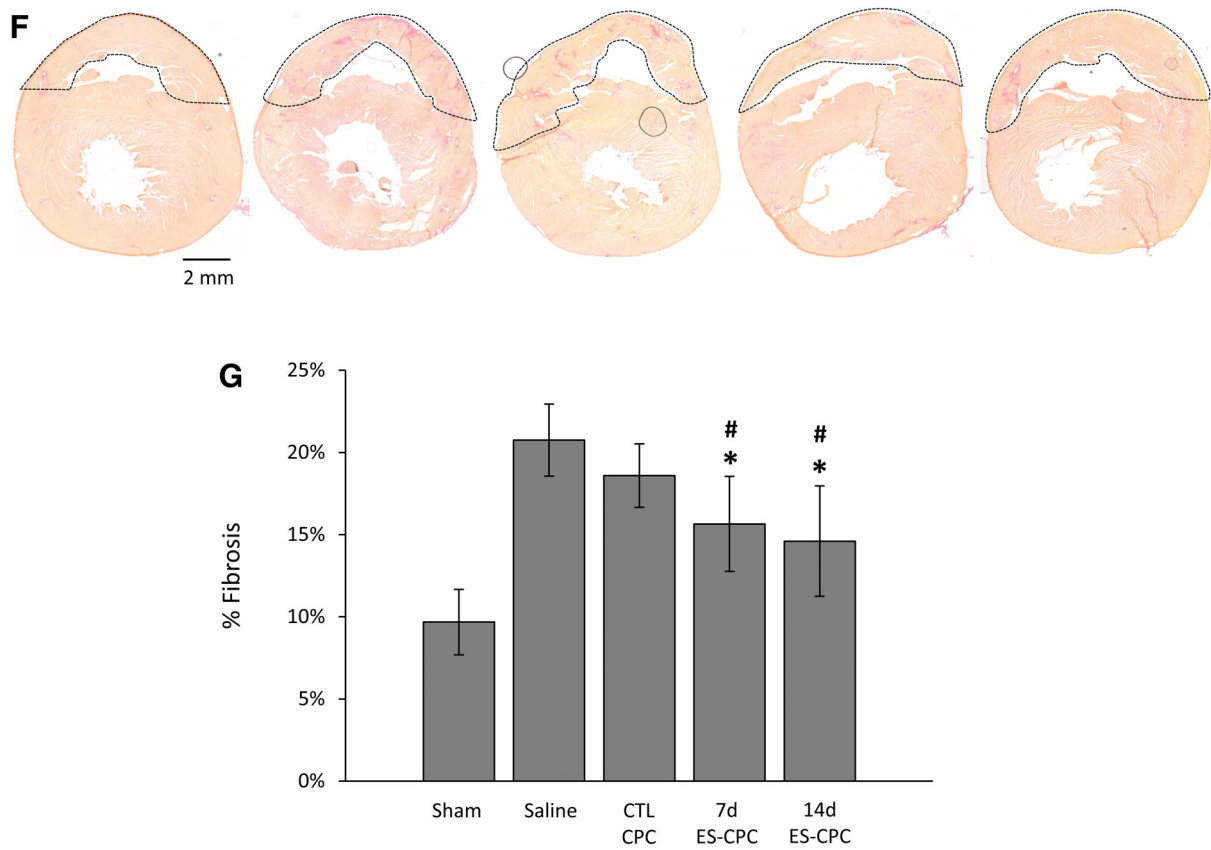
F

2 mm

G

% Fibrosis

Sham | Saline | CTL CPC | 7d ES-CPC | 14d ES-CPC

Figure 1. (Continued)

[30, 31]. We next examined whether ES induced the maturation of calcium oscillations toward Ca^{2+} transients seen in adult cardiac myocytes. In our previous publication, we show that ES induces a rapid rise in cytosolic Ca^{2+} followed by frequency independent cytosolic (and nuclear) Ca^{2+} oscillations [27]. Chronic ES did not induce maturation of calcium oscillation toward those seen in adult cardiac myocytes with 7- and 14-day Ca^{2+} oscillations not becoming frequency dependent and being nearly indistinguishable from those seen in acutely stimulated CPCs (Supporting Information Fig. S3 and Ref. [27]).

ES-CPCs Improve RV Function and Structure in PAB Rats

To test whether ES induces increases in the therapeutic efficacy of CPCs, we injected 7- and 14-day ES-CPCs into the right ventricular free wall of juvenile rats that had undergone PAB surgery. We and others have shown PAB rapidly induces hypertrophy and failure of the RV in rats, with RV functional parameters significantly reduced 2 weeks post-banding [7, 32–34]. Cells were injected 2 weeks post-banding, and echocardiography was performed biweekly for 6 weeks. Rats receiving either 7- or 14-day ES-CPCs showed significant improvement in critical RV functional and structural parameters over animal injected with saline or unmodified CPCs. As shown in Figure 1A, TAPSE was significantly increased in PAB animals receiving ES-CPCs 2 weeks post-injection compared with animals receiving saline or unmodified CPCs. We also observed significant decreases in right ventricular ejection time (Fig. 1B), right

ventricular wall thickness (Fig. 1C), and RVEDD (Fig. 1E) in animals receiving 7- or 14-day ES-CPCs when compared with animals receiving saline or control CPCs. Additionally, animals receiving 7- or 14-day ES-CPCs showed significantly increased right ventricular fractional area of contraction (Fig. 1D) when compared with animals receiving saline or control CPCs. We also quantified RV fibrotic area in hearts from PAB and sham rats with or without CPC injections. Rat hearts sections from animals injected with either 7- or 14-day ES-CPCs showed significantly less right ventricular free wall fibrotic area than animals receiving saline or control CPCs (Fig. 1E and F). We did not observe significant differences in the number of apoptotic cells as quantified by TUNEL staining at 42 days between sham, saline, control CPCs, and ES-CPC-treated hearts (Supporting Information Fig. S4).

Electrical Stimulation Improves CPC Myocardial Retention

To test the ability of CPCs to be retained in the myocardium, control and ES-CPCs were labeled with DiR prior to injection and fluorescence was tracked in vivo. ES-CPCs were retained at significantly higher amounts in the RV myocardium compared with control CPCs (Fig. 2A and B). Heart sections from PAB rats receiving ES-CPCs were probed with anti-Ku86 antibody to detect human cells. ES-CPCs were spread over areas of the RV free wall in the outermost layer of tissue or the epicardium (Fig. 2C and Supporting Information Figure S5). Cells were not localized in a bolus as could be expected after
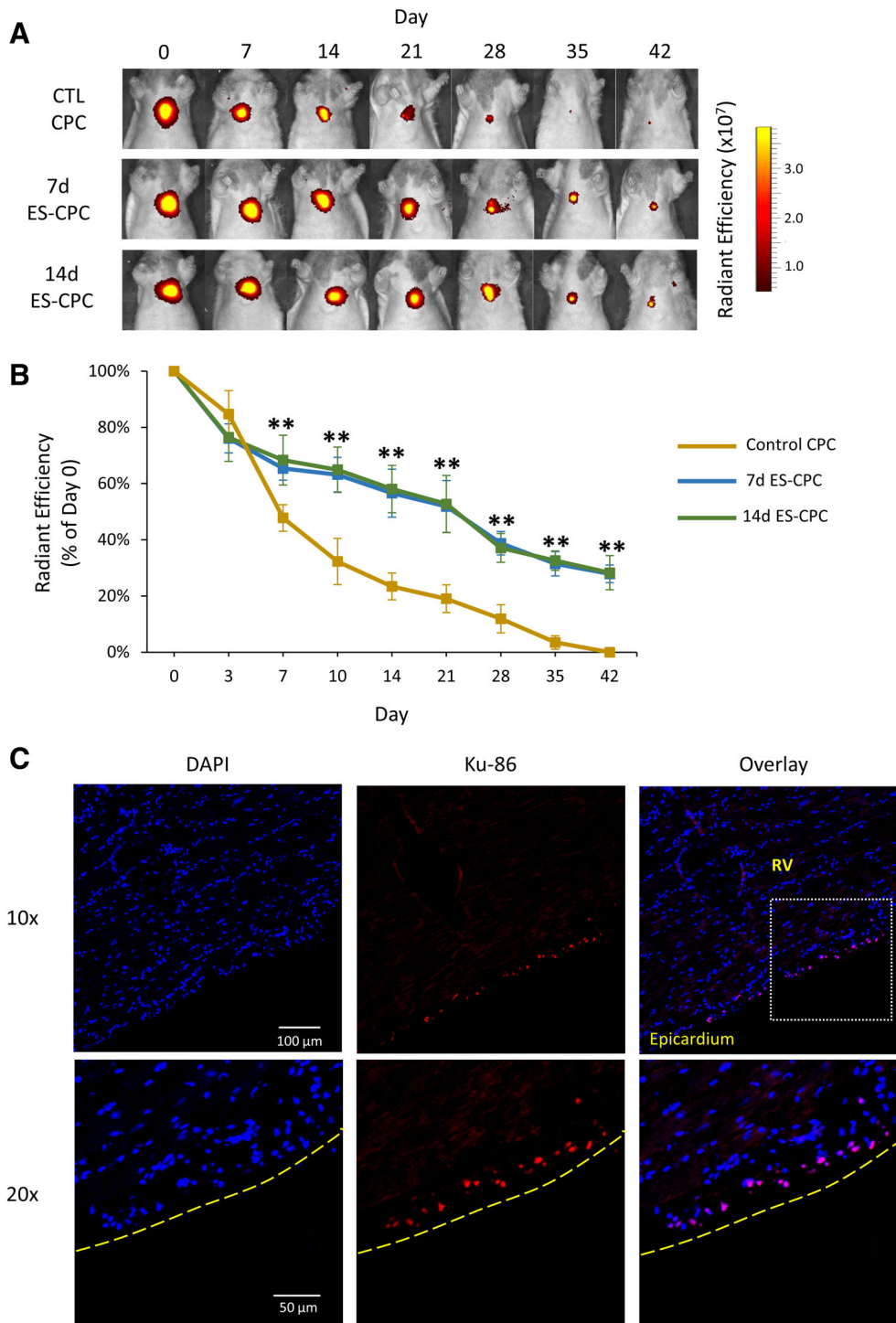
Figure 2. ES significantly improves the retention of CPCs in PAB hearts. **(A):** Representative in vivo DiR fluorescence images of rats injected with control or 7- or 14-day ES-CPCs. **(B):** Summary time course of fluorescence in PAB rats injected with DiR-labeled CPCs. Values are normalized to day 0 fluorescence values and plotted as percentage. $n = 9$ (control CPCs), $n = 9$ (7-day), $n = 7$ (14-day). Data are presented as mean $\pm$ SD. *, $p \leq .05$ vs. control CPCs. **(C):** Representative immunohistochemical staining images of heart sections from PAB rats injected with 7-day ES-CPCs. Images were acquired at 10× (top) and 20× (bottom). Dashed box in 10× represents 20× scan area. See also Supporting Information Figure S5. Abbreviations: CPCs, cardiac-derived c-kit+ progenitor cells; ES-CPCs, electrically stimulated CPCs; PAB, pulmonary artery banding.

injection, indicating that these cells are able to migrate to specific regions in the heart after delivery. Together, these data indicate that ES of human CPCs improves their therapeutic effect and increases their retention in the failing myocardium.

Of note, no significant difference was observed regarding improvements in RV function, structure, or CPC retention between 7- and 14-day ES-CPCs. Therefore, we continued with the time point of 7-day ES-CPCs for further analysis.
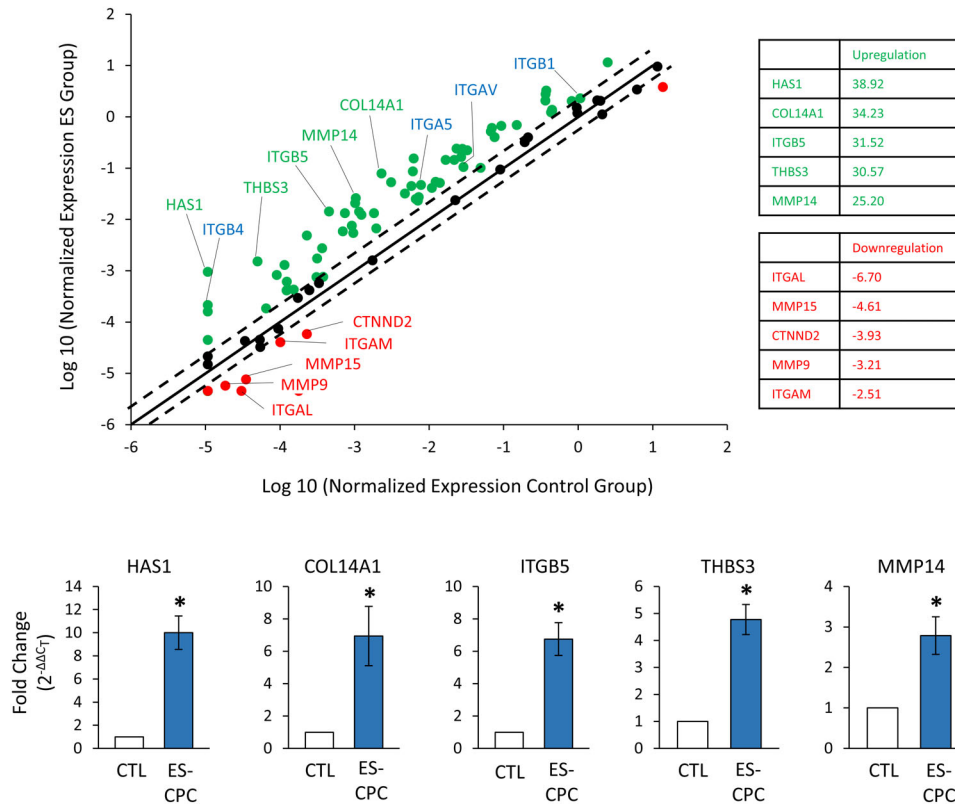
	Upregulation
HAS1	38.92
COL14A1	34.23
ITGB5	31.52
THBS3	30.57
MMP14	25.20

	Downregulation
ITGAL	-6.70
MMP15	-4.61
CTNND2	-3.93
MMP9	-3.21
ITGAM	-2.51

Figure 3. ES induces upregulation of extracellular matrix and cell adhesion genes in CPCs. **(A):** Scatter plot of gene array data from control and 7-day ES-CPCs showing upregulated (green), downregulated (red), and below threshold (black) genes between control and ES-CPCs. Dashed lines indicate ±two fold regulation threshold, and the solid line is unchanged gene expression. The top five upregulated and downregulated genes are shown in the inset table. **(B):** Summary qRT-PCR data of the fold change versus control of top five upregulated genes in ES-CPCs from the gene array data. N = 3. Data are presented as mean ± SD. *, $p \leq .05$ versus control. Abbreviations: CPCs, cardiac-derived c-kit^{+} progenitor cells; ES-CPCs, electrically stimulated CPCs; qRT-PCR, quantitative real-time polymerase chain reaction.
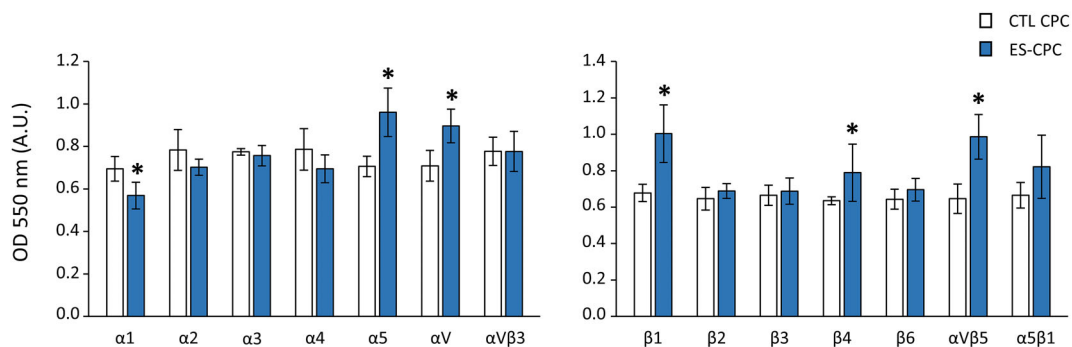

Figure 4. ES induces upregulation of integrin protein expression in CPCs. Summary graphs of alpha (left) and beta (right) integrin protein expression from control and ES-CPCs as quantified by colorimetric α/β integrin mediated cell adhesion array. n = 6. Data are presented as mean ± SD. *, $p \leq .05$ versus control. Abbreviations: CPCs, cardiac-derived c-kit^{+} progenitor cells; ES-CPCs, electrically stimulated CPCs.

ES Induces Upregulation of Key Extracellular Matrix and Adhesion Molecule Genes in CPCs

To begin dissecting the mechanism of increased ES-CPC retention in RV myocardium, we performed gene analysis on ES-CPCs using an initial mRNA array of 84 extracellular matrix and adhesion molecules. Analysis of these data show that of the 84 genes assayed, 60 of them were upregulated, whereas only 9 were downregulated and 15 unchanged. The top five upregulated and downregulated genes are shown in Figure 3 along with the scatter plot comparing the normalized expression of all 84 genes. Real-time PCR analysis verified that *HAS1, COL14A1, ITGB5, THBS3,* and *MMP14* transcripts were significantly upregulated in
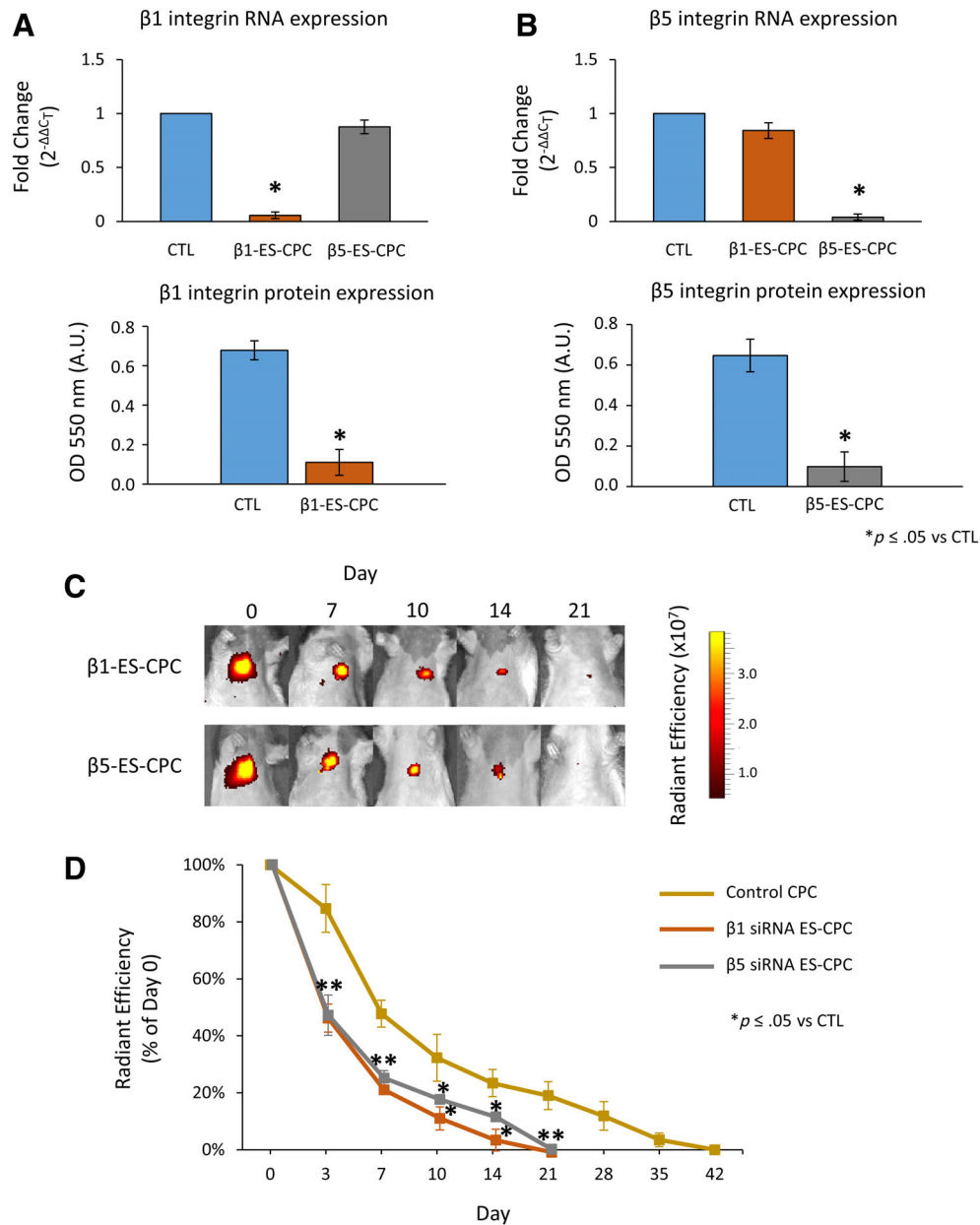
Figure 5. Upregulation of β1 and β5 integrins contribute to the increased retention of ES-CPCs. Summary graphs of **(A)** RT-PCR data and **(B)** protein expression array data from control CPCs and ES-CPCs transduced with β1 integrin shRNA (β1-ES-CPC) or β5 integrin shRNA (β5-ES-CPC) lentiviral vectors. **(C):** Representative in vivo DiR fluorescence images of rats injected with control or β1-ES-CPCs or β5-ES-CPCs. **(D):** Summary time course of fluorescence in PAB rats injected with DiR-labeled CPCs. Values are normalized to day 0 fluorescence values and plotted as percentage. n = 4–6. Data are presented as mean $\pm$ SD. *$p \leq$ .05 versus control. Abbreviations: CPCs, cardiac-derived c-kit$^+$ progenitor cells; ES-CPCs, electrically stimulated CPCs; PAB, pulmonary artery banding; RT-PCR, real-time polymerase chain reaction.

ES-CPCs compared with control CPCs. Together, these data suggest that ES increases the gene expression of many key extracellular matrix and adhesion molecules in CPCs.

ES Induces Upregulation of Integrin Proteins in CPCs

We next sought to examine and verify changes in integrin protein expression levels. We assayed the protein expression levels of common alpha and beta integrins by ELISA (Fig. 4). We found α5, αV, β1, β 4, and αVβ5 protein levels significantly upregulated in ES-CPCs compared with control. Integrin α1 was significantly downregulated in ES-CPCs compared with

control. Of note, the gene expression levels for all five of the proteins were also found to be significantly upregulated by gene array (see Fig. 3), with *ITGB5* (αVβ5 protein) being one of the top five upregulated genes. These data indicate that ES induces upregulation of multiple integrin proteins expression that may contribute to the retention of ES-CPCs.

β1 and β5 Integrins Contribute to the Increased Retention of ES-CPCs

We next aimed to determine if the upregulation of specific integrin proteins contributed to the increased retention of ES-
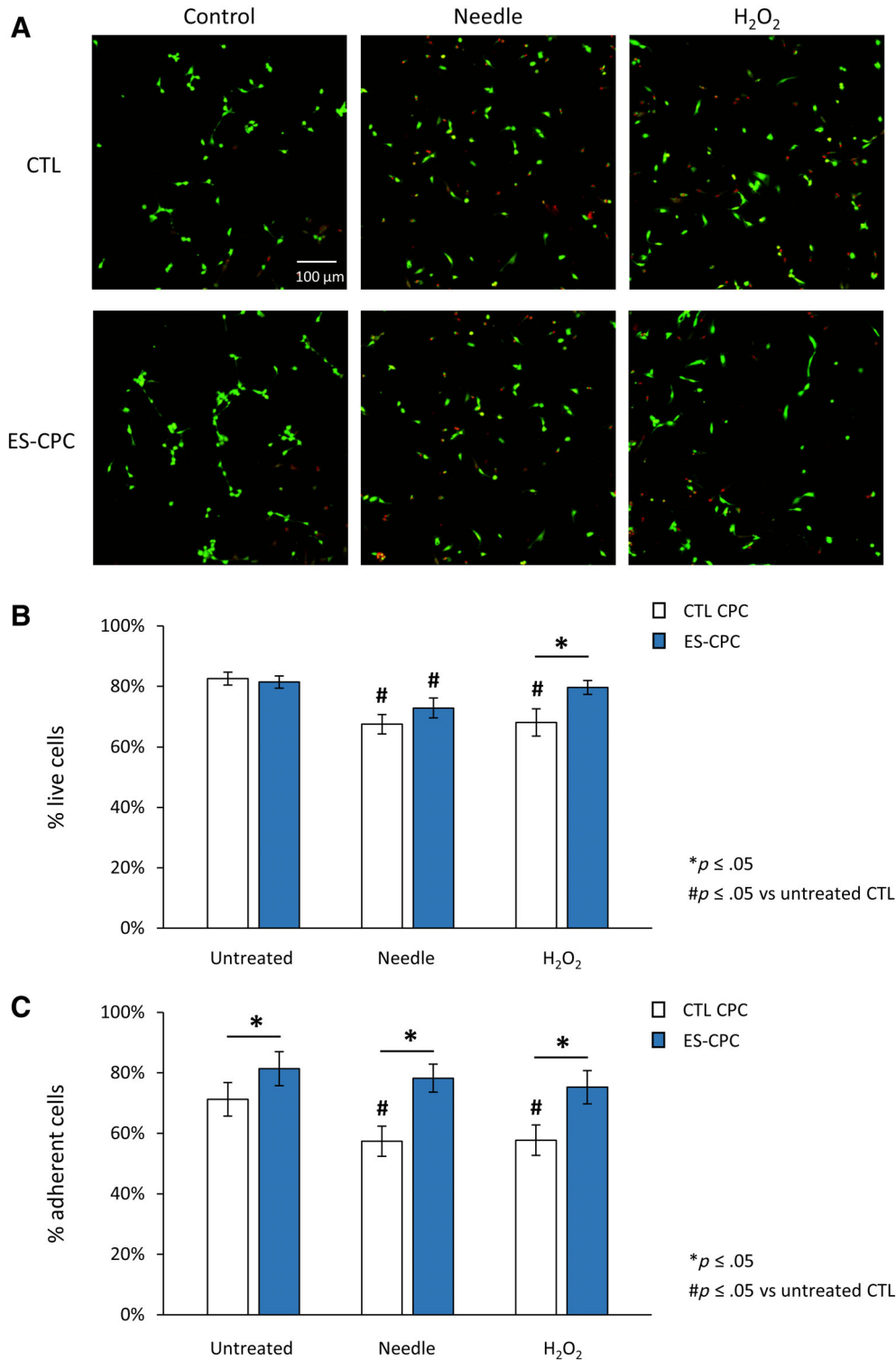
Figure 6. ES increases survival and adhesion of CPCs. **(A):** Representative immunocytochemical staining images of control and ES-CPCs under control conditions, after passage through a 27-gauge needle, or after 5 hours of treatment with 300 μM H_2O_2. Cells were stained with calcein (green) and ethidium homodimer-1 (red) to quantify live and dead cells under the various conditions. **(B):** Summary graph of live cell quantification from control (white) and ES-CPCs (blue) under the conditions show in **(A)**. $n = 4$. **(C):** Summary adherence data from control (white) and ES-CPCs (gray) under the conditions shown in **(A)** and quantified in a separate assay. $n = 5$. Data are presented as mean $\pm$ SD. *$p \leq .05$ vs. control, #$p \leq .05$ versus untreated. Abbreviations: CPCs, cardiac-derived c-kit$^+$ progenitor cells; ES-CPCs, electrically stimulated CPCs.

CPCs. We chose to examine the effect of β1 and β5 integrins on the in vivo retention of ES-CPCs because these were the two most upregulated integrins in response to ES (Fig. 4). We transduced CPCs with either β1- or β5-shRNA lentiviral vectors to inhibit expression of these integrins and then subjected the cells to our ES protocol for 7 days. The β1-shRNA transduced
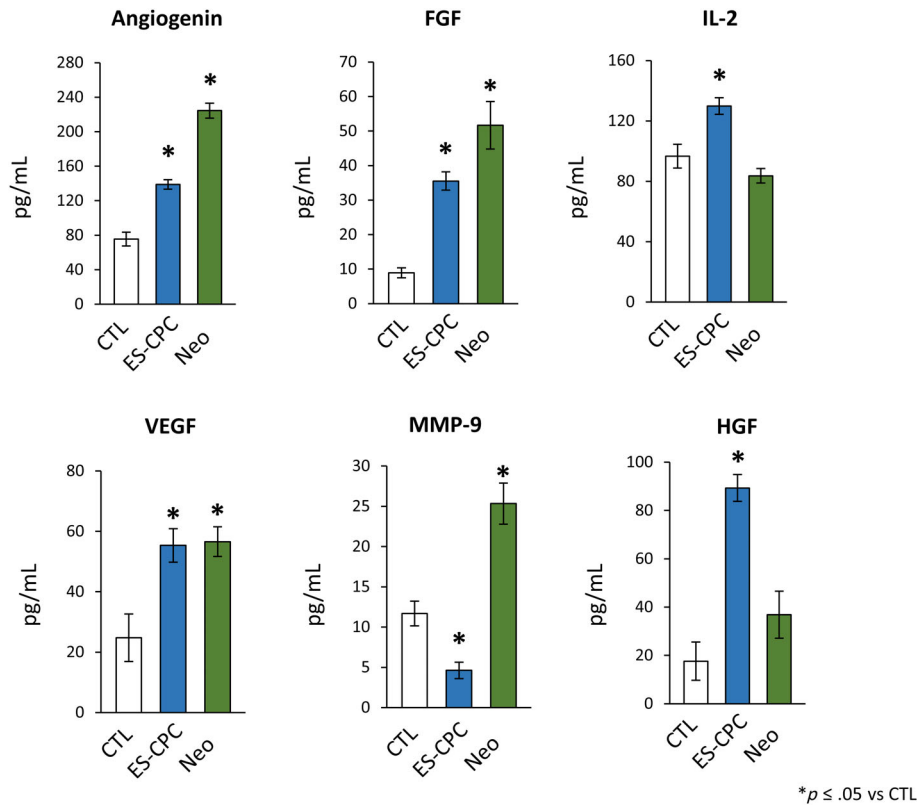
Figure 7. ES induces release of key paracrine factors from CPCs. Summary graphs of data from custom Luminex multiplex immunoassays of levels of select analytes released from control (white) and ES-CPCs (blue). *n* = 5. Data are presented as mean ± SD. *$p \leq .05$ versus control. Abbreviations: CPCs, cardiac-derived c-kit$^+$ progenitor cells; ES-CPCs, electrically stimulated CPCs.

ES-CPCs (β1-ES-CPCs) and the β5-shRNA transduced ES-CPCs (β5-ES-CPCs) showed corresponding reductions integrin RNA and protein levels (Fig. 5A-D). These cells were labeled with DiR, injected into the RV of PAB rats, and fluorescence was tracked in vivo. ES-CPCs exhibited significantly lower retention in the heart compared with control CPCs (Fig. 5E and F). We did not observe significant differences in the retention between β1-ES-CPCs and β5-ES-CPCs. These data suggest that the increased retention of ES-CPCs in the rat heart is in part due to the upregulation of integrins β1 and β5.

Survival and Adhesion

Previous studies have reported a pro-survival effect of ES on CPCs from mice [35]. We hypothesized that the increased retention of ES-CPCs we observed in vivo could be due to increased survival of ES-CPCs compared with control CPCs. Furthermore, our data indicated that increased extracellular adhesion protein expression could be contributing to the increased in vivo retention of ES-CPCs. To examine the pro-survival and pro-adhesive effects of ES on human CPCs, we performed survival and adhesion assays under various conditions using control and ES-CPCs. Control and ES-CPCs were assayed for survival and adherence under control conditions, after passage through a 27-gauge needle, or after exposure to 300 M H_2O_2 for 5 hours. We chose these conditions because the cells were injected into PAB rats with a 27-gauge needle, and the H_2O_2 will induce cytotoxicity in cells as the harsh environment of a failing or ischemic heart might [35]. Although passage through a needle and H_2O_2

treatment reduced survival of CPCs, we did not observe a significant protective effect after needle passage in the ES-CPCs. We did see significantly higher survival rates of ES-CPCs compared with control after H_2O_2 treatment (Fig. 6A and B). Passage through a needle and H_2O_2 treatment also reduced adhesion of control CPCs; however, significantly higher levels of cell adhesion were seen under all three conditions with ES-CPCs (Fig. 6C). In addition, there was no significant effect on the number of adherent ES-CPCs for the three conditions tested (control vs. needle vs. H_2O_2; *p* = .227). These data suggest that the increased adhesive properties of ES-CPCs are responsible for increased in vivo retention to a greater extent than the pro-survival effect of ES.

ES Increases Secretion of Pro-Reparative Molecules from CPCs

Recent studies have suggested that the mechanism of stem cell-mediated repair of the heart is through an indirect paracrine effect such as the release of reparative factors [36–40].

Therefore, we assessed the release of key soluble proteins by control and ES-CPCs. As shown in Figure 7, analysis of secreted analytes shows significantly increased release of Ang, FGF, IL-2, VEGF, and HGF in ES-CPCs compared with control. Additionally, MMP-9, a reported negative inotrope, was significantly decreased with ES [41] consistent with our gene array data (see Fig. 4). Previous work has shown neonatal CPCs to be the most effective at restoring RV function after PAB. These CPCs come from patients between 1 week and 1 month of age and have been hypothesized to exert their effects through a

paracrine mechanism. As such, we compared the levels of key soluble proteins from neonatal CPCs with ES-CPCs (Fig. 7). Interestingly, we observed the release profile of ES-CPCs to be more similar to neonatal CPCs than the control CPCs were. ES-CPCs released similar levels of VEGF as neonatal CPCs and had release levels of angiogenin and FGF that were approaching those of neonatal CPCs. These data indicate that ES increases the release of pro-reparative molecules from CPCs and provide insight into the mechanism of in vivo action of ES-CPCs.

DISCUSSION

The emergence of cardiovascular regenerative medicine as a potential therapeutic strategy for HF or myocardial infarction has provided new avenues for treatment with a focus on replacing or regenerating the damaged myocardium to restore normal cardiac function. Our results indicate that ES-CPCs have a greater reparative effect on the failing RV than control CPCs. Interestingly, our results revealed that ES significantly enhances the in vivo retention of CPCs compared with unstimulated cells. We found ES-CPCs to be primarily localized to the epicardial layer of hearts at 42 days post-injection and spread over the surface of the RV free wall. ES induced the expression of extracellular matrix and adhesion molecules, and we found the increased in vivo retention of ES-CPCs is in part due to the upregulation of integrins β1 and β5. Finally, we found the release of several key pro-reparative analytes to be increased in ES-CPCs, which may have a role in the enhanced functional improvement of RV function. Taken together, these results provide a novel method for enhancing the therapeutic effect of human CPCs for the treatment of cardiac pathologies.

Not only can our results be used to enhance future therapies with pediatric CPCs but the results could also be extrapolated to adult cells or to other stem cell types to enhance their reparative efficacy. Additionally, banking pediatric CPCs before or after ES will allow for an "off-the-shelf" allogeneic treatment for a broad range of cardiac pathologies. Allogeneic cardiac stem cell trials including ALLSTAR, DYNAMIC, POSEIDON-DCM, ALPHA, and CAREMI have illustrated the effectiveness and safety of allogeneic cardiac stem cells including CPCs in humans [42–44] with allogeneic cells performing better than autologous in some studies [45]. Importantly, many studies have shown that allogeneic CPCs do not elicit an immune response [46–49]. Additionally, our results are not limited to RV failure, as the in vivo mechanisms indicated by our data suggest that this may be a broader therapy for other cardiac indications including LV failure and myocardial infarction. Although we do show enhanced release of key analytes such as growth factors and modulators of the immune response, it is not clear from our results whether ES-CPCs are more reparative than control CPCs or if the functional effects we report are simply due to more cells being retained after injection. Previous work has shown neonatal CPCs to be the most effective at restoring RV function after PAB. These CPCs come from patients between 1 week and 1 month of age and have been hypothesized to exert their effects through a paracrine mechanism. Our data do indicate that ES can cause pediatric CPCs to release key soluble factors at levels similar to that of neonatal CPCs. Therefore, addressing the mechanism behind the improved reparative efficacy and the mechanism of action of ES-CPCs warrants further examination.

We obtained many interesting results from our extracellular matrix and adhesion molecule gene array analysis, many of which were corroborated by further investigation. The upregulation of multiple integrins was observed and confirmed by protein expression analysis. Of note, integrin β5 was found to be highly upregulated at the gene and protein levels and has been shown to be expressed on angiogenic endothelial cells and improve the reparative functions of endothelial progenitors within the cardiovascular system [50]. Integrin β5 has also been implicated in tissue angiogenesis and migration of tumor cells [51]. We also found integrin β1 to be upregulated at both the gene and protein levels. Integrin β1 has been shown to bind to fibronectin in vivo, and we reported that culturing CPCs on fibronectin is optimal for their VEGF A secretion, proliferation, connexin43 expression, and alignment [52]. Interestingly, fibronectin was also shown to induce proliferation and protection of CPCs in vivo and in vitro via β1 integrin-mediated signaling [53]. Integrin β1 has also been shown to be an essential stem cell niche molecule which cooperates with FGF to activate stem cell growth [54]. We found increased levels of FGF release from ES-CPCs compared with control cells, which may activate endogenous stem cell growth after cell injection and contribute to the increased functional effect of ES-CPCs. We also observed increased HGF release, which has been implicated in cardiac regeneration and CPC activation [55], decreased MMP-9 release, which has a negative effect on heart contractility [41], and increased angiogenin release, which has been shown to increase angiogenesis and improve LV function in myocardial infarction rat models [37, 56, 57]. The release of pro-angiogenic factors and localization to the epicardial layer in vivo suggest that ES may induce CPCs to differentiate toward an endothelial phenotype. However, despite upregulation of VCAM and ICAM gene expression via our gene array profiling, we did not detect PECAM expression via immunohistochemical staining of PAB heart slices nor was PECAM upregulated via gene array.

We have previously shown that ES induces oscillations in both cytosolic and nuclear Ca^{2+} in pediatric CPCs [27]. We hypothesize that it is likely that this activation of Ca^{2+} signaling is the cause of the substantial changes in gene expression we observe in ES-CPCs. Although not tested directly here, we envision that other activators of increased intracellular calcium may have the same effect as ES, and perhaps a more efficient way to activate the changes in gene expression can be found such as a more direct agonist of the activated Ca^{2+}-dependent signaling cascades or higher frequency ES. In general, many other "stress" environments, such as hypoxia and heat shock, have shown positive benefits to cardiac stem cell function [40, 58, 59]. Thus, it appears that many stressors may activate a pro-reparative gene expression profile in c-kit^{+} progenitor cells. It is also possible that treatment in these stress environments allow only the most healthy cells to survive. Selecting for only the most vigorous cells to be injected skews the in vivo data toward higher levels of retention and survival for the treatment groups. Although this is possible, our data indicate that the increased expression of adhesion molecules also contribute to the increased retention of ES-CPCs, specifically through β1 and β5 integrins. Additionally, improved ES-CPC retention may also be partly explained by our observation of significantly increased release of MMP9 and bFGF, factors that have been shown to promote cell engraftment and cell

survival [60, 61]. Further studies are required to determine the exact effect of the various ex vivo modifications on in vivo CPC function.

CONCLUSION

Together, these results reveal a potential method for improving the retention and function of cardiac stem cells. Our data indicate that ES improves CPC function, retention, and survival. We also provide insights into the mechanism of increased retention of ES-CPCs that has implications on a variety of stem cells and stem cell therapies. Future studies on the in vivo differentiation and function, such as release of paracrine factors including exosomes, of ES-CPCs will provide further insights into the mechanism of the enhanced reparative ability of these cells.

AUTHOR CONTRIBUTIONS

J.T.M.: conception and design, financial support, collection and assembly of data, data analysis and interpretation, manuscript writing, and final approval of manuscript; D.T.: collection and assembly of data, data analysis and interpretation, manuscript writing, and final approval of manuscript; M.S.: collection and assembly of data, data analysis and interpretation, final approval of manuscript; M.E.B.: collection and assembly of data, data analysis and interpretation, and final approval of manuscript; M.E.D.: data analysis and interpretation and final approval of manuscript; M.S.C.: collection and assembly of data, data analysis and interpretation, and final approval of manuscript; K.J.S.: collection and assembly of data, data analysis and interpretation, and final approval of manuscript; C.A.Z.: collection and assembly of data, data analysis and interpretation, and final approval of manuscript; E.B.: collection and assembly of data, data analysis and interpretation, and final approval of manuscript; M.L.L.: collection and assembly of data, data analysis and interpretation, and final approval of manuscript; J.Z.: collection and assembly of data, data analysis and interpretation, and final approval of manuscript; D.I.J.: collection and assembly of data, data analysis and interpretation, and final approval of manuscript.

DISCLOSURE OF POTENTIAL CONFLICTS OF INTEREST

The authors indicated no potential conflicts of interest.

DATA AVAILABILITY STATEMENT

The data that support the findings of this study are available from the corresponding author upon reasonable request.

REFERENCES

1 Jenkins KJ, Correa A, Feinstein JA et al. Noninherited risk factors and congenital cardiovascular defects: Current knowledge: A scientific statement from the American Heart Association Council on Cardiovascular Disease in the Young: Endorsed by the American Academy of Pediatrics. Circulation 2007;115: 2995–3014.

2 Guihaire J, Haddad F, Mercier O et al. The right heart in congenital heart disease, mechanisms and recent advances. J Clin Exp Cardiol 2012;8:1–11.

3 Strniskova M, Ravingerova T, Neckar J et al. Changes in the expression and/or activation of regulatory proteins in rat hearts adapted to chronic hypoxia. Gen Physiol Biophys 2006;25:25–41.

4 Wang GY, McCloskey DT, Turcato S et al. Contrasting inotropic responses to alpha1-adrenergic receptor stimulation in left versus right ventricular myocardium. Am J Physiol Heart Circ Physiol 2006;291: H2013–H2017.

5 Winter MM, Bouma BJ, Groenink M et al. Latest insights in therapeutic options for systemic right ventricular failure: a comparison with left ventricular failure. Heart 2009;95:960–963.

6 Orlic D, Kajstura J, Chimenti S et al. Bone marrow cells regenerate infarcted myocardium. Nature 2001;410:701–705.

7 Agarwal U, Smith AW, French KM et al. Age-dependent effect of pediatric cardiac progenitor cells after juvenile heart failure. STEM CELLS TRANSLATIONAL MEDICINE 2016;5: 883–892.

8 Norozi K, Gravenhorst V, Hobbiebrunken E et al. Normality of cardiopulmonary capacity in children operated on to correct congenital heart defects. Arch Pediatr Adolesc Med 2005;159:1063–1068.

9 Chang RK, Chen AY, Klitzner TS. Factors associated with age at operation for children with congenital heart disease. Pediatrics 2000;105:1073–1081.

10 Jacobs JP, O'Brien SM, Pasquali SK et al. The Society of Thoracic Surgeons Congenital Heart Surgery Database mortality risk model: Part 2—Clinical application. Ann Thorac Surg 2015;100:1063–1070.

11 Roos-Hesselink JW, Meijboom FJ, Spitaels SEC et al. Long-term outcome after surgery for pulmonary stenosis (a longitudinal study of 22–33 years). Eur Heart J 2006;27: 482–488.

12 Pozzi M, Trivedi DB, Kitchiner D et al. Tetralogy of Fallot: what operation, at which age∗. Eur J Cardiothorac Surg 2000;17: 631–636.

13 Dai Y, Xu M, Wang Y et al. HIF-1alpha induced-VEGF overexpression in bone marrow stem cells protects cardiomyocytes against ischemia. J Mol Cell Cardiol 2007;42: 1036–1044.

14 Haider H, Sim EK, Lei Y et al. Cell-based ex vivo delivery of angiogenic growth factors for cardiac repair. Arterioscler Thromb Vasc Biol 2005;25:e144.

15 Mangi AA, Noiseux N, Kong D et al. Mesenchymal stem cells modified with Akt prevent remodeling and restore performance of infarcted hearts. Nat Med 2003;9:1195–1201.

16 Noiseux N, Gnecchi M, Lopez-Ilasaca M et al. Mesenchymal stem cells overexpressing Akt dramatically repair infarcted myocardium and improve cardiac function despite infrequent cellular fusion or differentiation. Mol Ther 2006;14:840–850.

17 Fischer KM, Cottage CT, Wu W et al. Enhancement of myocardial regeneration through genetic engineering of cardiac progenitor cells expressing Pim-1 kinase. Circulation 2009;120:2077–2087.

18 Christoforou N, Gearhart JD. Stem cells and their potential in cell-based cardiac therapies. Prog Cardiovasc Dis 2007;49:396–413.

19 Gnecchi M, He H, Noiseux N et al. Evidence supporting paracrine hypothesis for Akt-modified mesenchymal stem cell-mediated cardiac protection and functional improvement. FASEB J 2006;20:661–669.

20 Haider H, Ashraf M. Strategies to promote donor cell survival: combining preconditioning approach with stem cell transplantation. J Mol Cell Cardiol 2008;45: 554–566.

21 Deb KD, Sarda K. Human embryonic stem cells: Preclinical perspectives. J Transl Med 2008;6:7.

22 Llucià-Valldeperas A, Sanchez B, Soler-Botija C et al. Physiological conditioning by electric field stimulation promotes cardiomyogenic gene expression in human

cardiomyocyte progenitor cells. Stem Cell Res Ther 2014;5:93.

23 Llucià-Valldeperas A, Sanchez B, Soler-Botija C et al. Electrical stimulation of cardiac adipose tissue-derived progenitor cells modulates cell phenotype and genetic machinery. Journal of Tissue Engineering and Regenerative Medicine. 2015;9:E76–E83.

24 Pietronave S, Zamperone A, Oltolina F et al. Monophasic and biphasic electrical stimulation induces a precardiac differentiation in progenitor cells isolated from human heart. Stem Cells Dev 2014;23:888–898.

25 Serena E, Figallo E, Tandon N et al. Electrical stimulation of human embryonic stem cells: Cardiac differentiation and the generation of reactive oxygen species. Exp Cell Res 2009;315:3611–3619.

26 Gautam M, Fujita D, Kimura K et al. Transplantation of adipose tissue-derived stem cells improves cardiac contractile function and electrical stability in a rat myocardial infarction model. J Mol Cell Cardiol 2015;81:139–149.

27 Maxwell JT, Wagner MB, Davis ME. Electrically Induced Calcium Handling in Cardiac Progenitor Cells. Stem Cells Int 2016;2016:8917380:1–11.

28 French KM, Davis ME. Isolation and expansion of c-kit-positive cardiac progenitor cells by magnetic cell sorting. Methods Mol Biol 2014;1181:39–50.

29 Sultana N, Zhang L, Yan J et al. Resident c-kit(+) cells in the heart are not cardiac stem cells. Nat Commun 2015;6:8701.

30 Ruijtenberg S, van den Heuvel S. Coordinating cell proliferation and differentiation: Antagonism between cell cycle regulators and cell type-specific gene expression. Cell Cycle 2016;15:196–212.

31 Segers VF, Lee RT. Stem-cell therapy for cardiac disease. Nature 2008;451:937–942.

32 Trac D, Maxwell JT, Brown ME et al. Aggregation of child cardiac progenitor cells into spheres activates notch signaling and improves treatment of right ventricular heart failure. Circ Res 2019;124:526–538.

33 Maxwell JT, Somasuntharam I, Gray WD et al. Bioactive nanoparticles improve calcium handling in failing cardiac myocytes. Nanomedicine 2015;10:3343–3357.

34 Oommen S, Yamada S, Cantero Peral S et al. Human umbilical cord blood-derived mononuclear cells improve murine ventricular function upon intramyocardial delivery in right ventricular chronic pressure overload. Stem Cell Res Ther 2015;6:50.

35 Kim SW, Kim HW, Huang W et al. Cardiac stem cells with electrical stimulation improve ischaemic heart function through regulation of connective tissue growth factor and miR-378. Cardiovasc Res 2013;100:241–251.

36 Maxeiner H, Krehbiehl N, Muller A et al. New insights into paracrine mechanisms of human cardiac progenitor cells. Eur J Heart Fail 2010;12:730–737.

37 Hsiao ST, Lokmic Z, Peshavariya H et al. Hypoxic conditioning enhances the angiogenic paracrine activity of human adipose-derived stem cells. Stem Cells Dev 2013;22:1614–1623.

38 Mayourian J, Ceholski DK, Gorski P et al. Exosomal microRNA-21-5p mediates mesenchymal stem cell paracrine effects on human cardiac tissue contractility. Circ Res 2018;122:933–944.

39 Agarwal U, George A, Bhutani S et al. Experimental, systems, and computational approaches to understanding the microRNA-mediated reparative potential of cardiac progenitor cell-derived exosomes from pediatric patients. Circ Res 2017;120:701–712.

40 Gray WD, French KM, Ghosh-Choudhary S et al. Identification of therapeutic covariant microRNA clusters in hypoxia-treated cardiac progenitor cell exosomes using systems biology. Circ Res 2015;116:255–263.

41 Prathipati P, Metreveli N, Nandi SS et al. Ablation of matrix metalloproteinase-9 prevents cardiomyocytes contractile dysfunction in diabetics. Front Physiol 2016;7:93–109.

42 Chakravarty T, Makkar RR, Ascheim DD et al. ALLogeneic heart stem cells to achieve myocardial regeneration (ALLSTAR) trial: Rationale and design. Cell Transplant 2017;26:205–214.

43 Sanz-Ruiz R, Casado Plasencia A, Borlado LR et al. Rationale and design of a clinical trial to evaluate the safety and efficacy of intracoronary infusion of allogeneic human cardiac stem cells in patients with acute myocardial infarction and left ventricular dysfunction: The randomized multicenter double-blind controlled CAREMI trial (cardiac stem cells in patients with acute myocardial infarction). Circ Res 2017;121:71–80.

44 Crisostomo V, Casado JG, Baez-Diaz C et al. Allogeneic cardiac stem cell administration for acute myocardial infarction. Expert Rev Cardiovasc Ther 2015;13:285–299.

45 Hare JM, DiFede DL, Rieger AC et al. randomized comparison of allogeneic versus autologous mesenchymal stem cells for non-ischemic dilated cardiomyopathy: POSEIDON-DCM trial. J Am Coll Cardiol 2017;69:526–537.

46 Lauden L, Boukouaci W, Dam N et al. 39-OR: Allogenicity of human cardiac stem/progenitor cells. Hum Immunol 2013;74:30.

47 Weng Y, Zhang X, Liu A et al. The effect of allogeneic cardiac stem cells in left ventricular geometry and function in a rat model of myocardial infarction. Cardiovasc Ther 2018;36:e12313.

48 Hocine HR, Costa HE, Dam N et al. Minimizing the risk of allo-sensitization to optimize the benefit of allogeneic cardiac-derived stem/progenitor cells. Sci Rep 2017;7:41125.

49 Sanz-Ruiz R, Fernández-Avilés F. Autologous and allogeneic cardiac stem cell therapy for cardiovascular diseases. Pharmacol Res 2018;127:92–100.

50 Leifheit-Nestler M, Conrad G, Heida NM et al. Overexpression of integrin beta 5 enhances the paracrine properties of circulating angiogenic cells via Src kinase-mediated activation of STAT3. Arterioscler Thromb Vasc Biol 2010;30:1398–1406.

51 Bianchi-Smiraglia A, Paesante S, Bakin A. Integrin β5 contributes to the tumorigenic potential of breast cancer cells through Src-FAK and MEK-ERK signaling pathways. Oncogene 2013;32:3049–3058.

52 French KM, Maxwell JT, Bhutani S et al. Fibronectin and cyclic strain improve cardiac progenitor cell regenerative potential in vitro. Stem Cells Int 2016;2016:8364382.

53 Konstandin MH, Toko H, Gastelum GM et al. Fibronectin is essential for reparative cardiac progenitor cell response after myocardial infarction. Circ Res 2013;113:115–125.

54 Rozo M, Li L, Fan CM. Targeting beta1-integrin signaling enhances regeneration in aged and dystrophic muscle in mice. Nat Med 2016;22:889–896.

55 Gallo S, Sala V, Gatti S et al. HGF/Met axis in heart function and cardioprotection. Biomedicine 2014;2:247.

56 Liu XH, Bai CG, Xu ZY et al. Therapeutic potential of angiogenin modified mesenchymal stem cells: angiogenin improves mesenchymal stem cells survival under hypoxia and enhances vasculogenesis in myocardial infarction. Microvasc Res 2008;76:23–30.

57 Ascione R, Rowlinson J, Avolio E et al. Migration towards SDF-1 selects angiogenin-expressing bone marrow monocytes endowed with cardiac reparative activity in patients with previous myocardial infarction. Stem Cell Res Ther 2015;6:53.

58 Feng Y, Huang W, Meng W et al. Heat shock improves Sca-1+ stem cell survival and directs ischemic cardiomyocytes toward a prosurvival phenotype via exosomal transfer: a critical role for HSF1/miR-34a/HSP70 pathway. STEM CELLS 2014;32:462–472.

59 Qiao P-F. Heat shock pretreatment improves stem cell repair following ischemia-reperfusion injury via autophagy 2015. World J Gastroenterol. 21: 12822–12834.

60 Shen D, Tang J, Hensley MT et al. Effects of matrix metalloproteinases on the performance of platelet fibrin gel spiked with cardiac stem cells in heart repair. Stem Cells Translational Medicine 2016;5:793–803.

61 Li Z, Guo X, Guan J. A thermosensitive hydrogel capable of releasing bFGF for enhanced differentiation of mesenchymal stem cell into cardiomyocyte-like cells under ischemic conditions. Biomacromolecules 2012;13:1956–1964.

See www.StemCells.com for supporting information available online.